Electrostatic height modulation of bound particle labels by buffer exchange in an evanescent wave biosensor

Electrostatic height modulation of bound particle labels by buffer exchange in an evanescent wave biosensor

Kim van Ommering,[1,2] Rik Paesen,[2] Hans B. A. van Zon,[1] Marjo Koets,[1] Leo J. van IJzendoorn,[2] and Menno W. J. Prins[1,2,a)]
[1]*Philips Research Laboratories, 5656 AE Eindhoven, The Netherlands*
[2]*Department of Applied Physics, Eindhoven University of Technology, 5600 MB Eindhoven, The Netherlands*

(Received 10 February 2010; accepted 24 June 2010; published online 10 August 2010)

We introduce a technique to electrostatically modulate the height of bound particle labels on a biosensor surface by exchanging the buffer. In an evanescent wave biosensor, height modulation leads to a modulation of the scattered and reflected light intensity. We measured a lower scattering and, therefore, a higher reflection for a decreasing ionic strength, which can be explained by an increasing electrostatic force repelling bound particles from the surface. By comparing bonds with troponin, 105 base pair (bp) DNA and 290 bp DNA, we found that the signal change for an ensemble of bound particles was related to the length of the analyte. Additionally, we observed for individual particles that the thermal fluctuations of scattered light intensity became smaller for decreasing ionic strength and that the average intensity shifted toward lower values, corresponding to larger particle heights. A quantitative model comprising electrostatic repulsion and van der Waals interaction could fit the measured height displacements for four different DNA lengths (105 bp to 590 bp) as analytes. Height manipulation of bound particle labels thus reflects analyte-specific properties and may lead to biosensors with enhanced specificity. © *2010 American Institute of Physics*. [doi:10.1063/1.3466985]

I. INTRODUCTION

Nanoparticles and microparticles are extensively being investigated as labels in biosensors.[1–3] Detection of analyte molecules takes place by binding the analyte to a biologically activated particle and detecting the concentration of bound particles in bulk or near a sensor surface. A detection principle that has recently been demonstrated to achieve low detection limits in short measurement times is the optomagnetic immunoassay, comprising magnetic particle labels and optical evanescent wave detection.[4] The detection limit in such a biosensor is influenced by the accuracy of measuring the particle concentration at the surface and by the error induced when not every detected particle corresponds to a specific analyte molecule.

The possibility to measure the mobility of bound particles is well-known from tethered particle motion experiments, where the measured Brownian motion of a bound particle gives information on the length and flexibility of the bond.[5,6] Techniques to actively manipulate the height of a bound particle are optical tweezers,[7–9] magnetic tweezers,[10–13] fluidic forces,[14,15] or methods in which the particle is attached to larger objects such as in atomic force microscopy or in a bioforce probe.[16] The challenge in manipulating particle height in a biosensor lies in exerting high, well-defined and uniform forces, preferably perpendicular to the surface, on large ensembles of particles. Although magnetic tweezers have been shown to be successful,[12,13] magnetic manipulation is limited, for example, by the force magnitude,[12] by magnetic interactions between particles, or by particle alignment due to magnetic anisotropy.[17]

It has been shown that the height of bound particles depends, among others, on the electrostatic force between the particle and the surface,[15] which in turn depends on the properties of the fluid in which they are immersed.[18] In this paper we describe a technique to modulate the height of bound particle labels in an evanescent wave biosensor by a fluidic buffer exchange. Because the evanescent field intensity decays exponentially with the distance to the surface,[19,20] height modulation of bound particles in an evanescent wave biosensor leads to a modulation of the detected signal. In future biosensor generations, this may lead to enhanced detection specificity because the amplitude of height modulation is expected to differ for different types of analytes.

II. MATERIALS AND METHODS

Electrostatic modulation of bound particles by buffer exchange is possible because of a surface charge which is present on both the particle and the sensor surface [Fig. 1(a)]. In high-salt buffers suitable for immunoassays, the surface charges are largely shielded by buffer ions, therefore, the electrostatic force between the particle and the surface is small. However, by decreasing the ionic strength of the buffer, the electrostatic force is increased and the particle is repelled from the surface. Figure 1(b) shows the theoretical change in interaction energy for decreasing ionic strength. With this technique, high repulsive forces can be induced, up to tens of piconewtons on 500 nm particles and particle-to-

a)Electronic mail: menno.prins@philips.com.

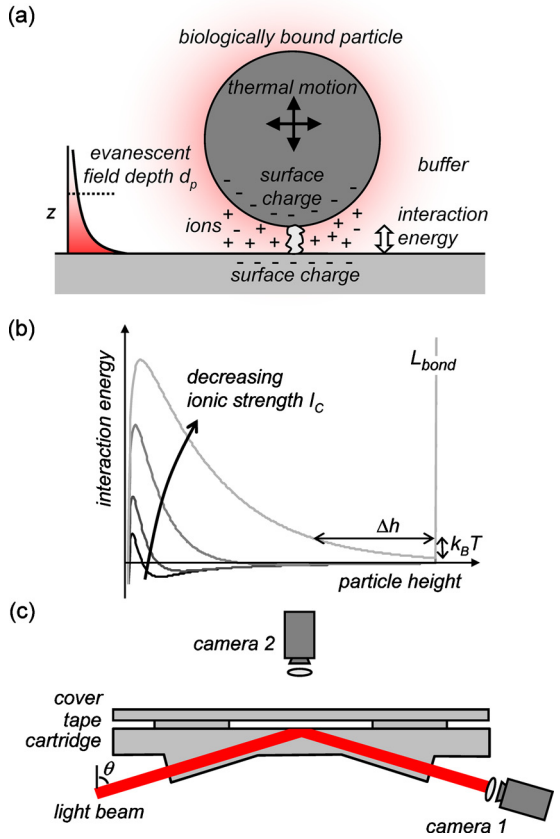

FIG. 1. (Color online) (a) Mobility of a bound particle due to thermal energy, generating intensity fluctuations by light scattering in an evanescent field. The particle and the sensor surface have a surface charge, leading to an electrostatic interaction. The surface charges are partly shielded by buffer ions. (b) Interaction energy between particle and surface, comprising the van der Waals energy and the electrostatic energy and the energy induced by the bond with length L_{bond}. The particle height fluctuations are determined by the thermal energy k_BT and the ionic strength I_C of the buffer. (c) Cross-section of the fluidic cartridge. Camera 1 measures the intensity of the reflected beam and camera 2 measures the scattered light from the cartridge surface.

particle interaction is small because electrostatic forces decrease exponentially and can be disregarded over a few hundred nanometers.

Figure 1(c) shows the evanescent wave biosensor setup. A light beam irradiates the surface of an injection-molded, polystyrene cartridge in a condition of total internal reflection, generating an optical evanescent field that penetrates into the fluid by a subwavelength distance.[4] Bound particle labels in the evanescent field scatter part of the light and thereby frustrate the total internal reflection, leading to a reduction in light intensity of the reflected beam and an increase in scattered light intensity from the sensor surface. Both signals are measured using lenses and charge coupled device camera's. When detecting the reflected signal (camera 1) we use a high power light-emitting diode as a light source (620–645 nm, Luxeon LXHL-BD03) and when detecting the scattered signal (camera 2) we use a laser diode (658 nm, Sanyo DL-6147-240, 20 mW) slightly focused onto the sensor surface to a 200 μm optical spot. In the latter case we obtain single-particle resolution using a microscope objective with high magnification (50×, NA=0.50, Leica N plan). The cartridge surface is coated with antibodies using an ink-jet printer (200 μm spots) and blocked in phosphate buffered saline (PBS) containing 1% (w/v) bovine serum albumin (BSA), 10% (w/v) sucrose, and 0.1% (w/v) sodium azide. For the reflected signal detection we create a fluidic channel using 180 μm double-sided tape and an injection-molded polystyrene cover with fluidic inlets; for the scattered signal detection we use 180 μm double-sided tape and a 150 μm thick cover glass. We use analyte molecules of different lengths: cardiac troponin I (cTnI) (Ref. 4) and four lengths of dsDNA amplicons 105 base pair (bp)/36 nm, 141 bp/48 nm, 290 bp/99 nm, and 509 bp/201 nm),[17,21] and we use two types of magnetic particles as labels: Ademtech Masterbeads with a diameter of 500 nm and MagSense beads with a diameter of 500 nm. In a one-step assay, troponin is bound via anti-cTnI goat polyclonal antibodies to the sensor surface and via tracer anti-cTnI monoclonal antibodies to the particles.[4] The DNA amplicons are tagged with Texas red and biotin, which bind in a one-step assay to antibodies against Texas red on the sensor surface and to streptavidin on the particles. We use low analyte concentrations (in solution are 0.3–3 analyte molecules per magnetic particle) and short incubation times (<5 min) in order to have a high probability of single-tether attachment.[18] Assay details can be found in Bruls *et al.*,[4] and van Ommering *et al.*[17]

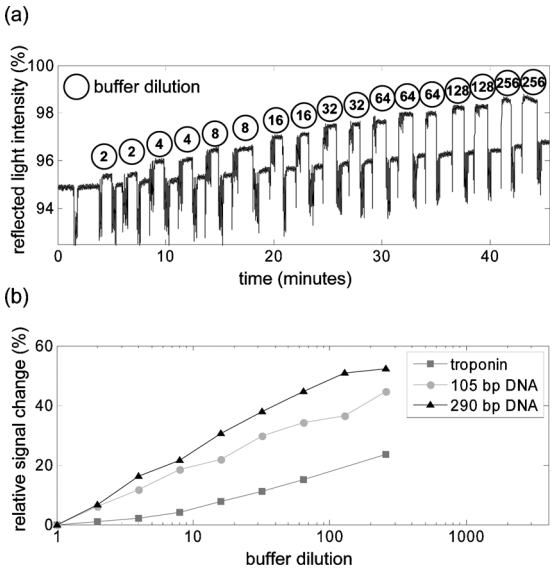

FIG. 2. (a) Measured intensity of the beam reflected from the sensor surface where particles are bound via 290 bp DNA. By replacing the buffer by diluted buffers (2, 4, 8, 16, 32, 64, 128, and 256 times diluted) the intensity signal is modulated. After flushing in a diluted buffer, the buffer is first replaced by the original buffer before further decreasing the buffer dilution. (b) Relative signal change as function of the buffer dilution [$100\%(s_{DB}-s_{OB})/(100\%-s_{OB})$, with s_{OB} the reflected signal in the original buffer and s_{DB} the reflected signal in the diluted buffer], for three types of analytes: troponin, 105 bp dsDNA and 290 bp dsDNA.

III. RESULTS AND DISCUSSION

Figure 2(a) shows a measurement of the reflected light [camera 1, Fig. 1(c)] from a surface containing Ademtech magnetic particles bound to 290 bp DNA. Unbound particles are washed away using a 100 mM borate buffer (*p*H 8.5) containing 0.05% (v/v) Tween 20. The resulting signal of the reflected light beam, measured on a spot on the sensor sur-

face of 75×75 μm, is 94.9%, corresponding approximately to (0.5 ± 0.2) particles/μm^2. When replacing the 100 mM borate buffer with a two times diluted buffer, we measured an increase in reflected signal from 94.9% to 95.4%. This can be explained by the decrease in ionic strength, leading to an increase in particle height, a decrease in scattered intensity per particle and thus an increase in reflected light. Next, we replaced the diluted buffer with the original (100 mM) buffer and saw that the signal returned to 94.9%, showing that the process is reversible and not due to removal of bound particles. We repeated this process for increasing buffer dilutions (2, 4, 8, 16, 32, 64, 128, and 256 times diluted) and observed that the steps in signals became larger for decreasing ionic strength, as can be expected from the increasing electrostatic force between particle and surface. Only after repeatedly replacing the buffers, we saw a small increase in the base signal due to removal of bound particles but this effect was negligible compared to the signal change by buffer replacement. Figure 2(a) also shows that when flushing in a buffer (diluted or original), a transient downward signal is observed, which we attribute to fluidic forces pushing particles toward the surface.[15,18] For higher buffer dilutions, the transient signal becomes smaller, showing that there is a higher repulsive force acting on the particles.

In Fig. 2(b) we plotted the relative signal change as a function of the buffer dilution for three types of analytes: troponin (~5–10 nm), 105 bp (36 nm) DNA and 290 bp (99 nm) DNA. For the troponin assay the dilutions were made from PBS buffer; for the DNA assay the dilutions were made from 100 mM borate buffer (pH 8.5) containing 0.05% (v/v) Tween 20. Figure 2(b) shows for all analytes an increase in relative signal change for increasing buffer dilution. Moreover, Fig. 2(b) also shows that the relative signal change depends on the bond length, as the smallest analyte troponin gives the lowest relative signal change and the largest analyte 290 bp DNA gives the largest relative signal change. For all analytes we observe a nearly linear dependence of the signal change on the logarithm of the buffer dilution.

The signal change in diluted buffers can be attributed to three successive mechanisms: (1) the buffer changes the electrostatic force on the particles, (2) the force changes the average particle height, and (3) the particle displacement changes the optical signal. To quantitatively analyze the intensity signal changes and relate these to the theory of electrostatic interaction between a particle and a surface, we modified the detection system by going to single-particle resolution and high-temporal resolution [camera 2, Fig. 1(c)]. In addition, we substituted the Ademtech magnetic particles for the optically more uniform MagSense magnetic particles. We have previously shown that measuring the thermally induced intensity fluctuations of single, optically uniform particles leads to accurate measurements of the height distribution of the particles.[22]

The histogram of the measured scattered intensity (30 s measurement at 60 Hz, exposure time of 1 ms) of the images of a single MagSense particle bound to 290 bp DNA is shown in Fig. 3(a). This figure shows that when replacing the 100 mM buffer with diluted buffers (2, 4, 8, 16, 32, 64, 128, and 256 times), the intensity histograms of the particle become narrower and the peak shifts toward lower intensity values corresponding to larger particle heights, showing that the particle is pushed away from the surface. We repeated this measurement for four particles, each bound to DNA of a different length. For each particle, we calculated the maximum height displacement $\Delta h = d_p \ln(I_{\max}/I_{\min})$, where d_p is the penetration depth of the evanescent field (95 nm in our setup[22]), and $I_{\max}$ and $I_{\min}$ are the maximum and minimum intensity values for which the measured probability decreases below 8%, equivalent to a thermal energy larger than 2.5 k_BT. In Fig. 3(b) the maximum height displacement of the four particles is plotted as a function of the buffer molarity.

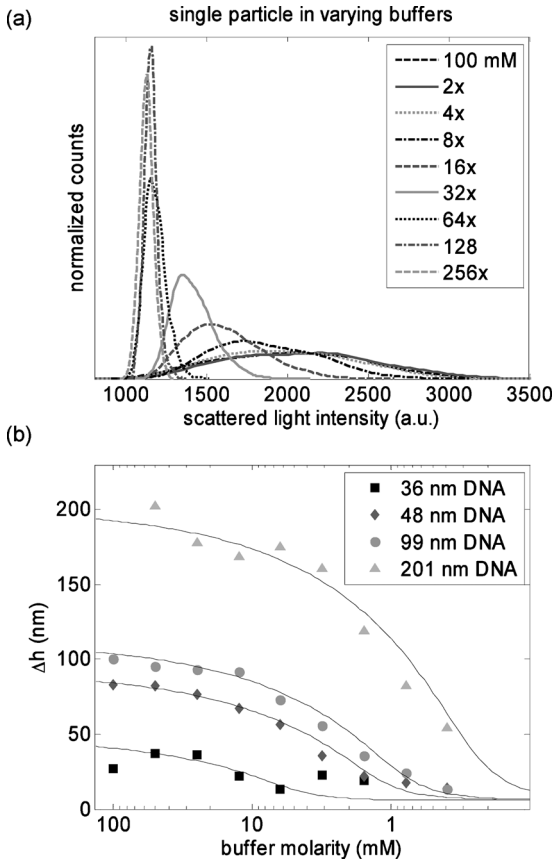

FIG. 3. (a) Histograms of the measured scattered intensity of a single MagSense particle bound to 290 bp DNA in different buffer conditions (2, 4, 8, 16, 32, 64, 128, and 256 times diluted), showing narrowing of the histograms for lower ionic strength and shifting of the peak toward lower intensity values. (b) Maximum height displacement of four particles, each bound to DNA of a different length, as function of the buffer molarity. The maximum height displacement is calculated from the minimum and maximum intensity of the intensity histograms.

To test the reproducibility of the experiments we measured for several particles a dilution series and additionally the same dilution series in reverse order, and observed that the results were identical for both series. It should be noted that at the start of an experiment we selected the best particles (~20%) based on symmetry of the intensity-position plots to exclude cases of (additional) nonspecific sticking.[17,23] Particles with slightly less symmetry in the intensity-position plots showed lower height displacements but still the same trend in the histograms for diluted buffers (narrowing and shifting of the peak). Finally, we note that

buffer replacement in the scattered intensity detection setup (using a cover glass instead of an injection-molded polystyrene cover) generates higher fluidic forces and, therefore, leads to a substantial increase in the loss of bound particles in the fluidic wash steps (more than half of the particles over several wash steps).

As a model for the energy of a bound particle, we combined the van der Waals energy and electrostatic energy (see the Appendix), and added a basic step function for the bond energy ($E=0$ for $h \leq L_{\text{bond}}$ and $E=\infty$ for $h > L_{\text{bond}}$). This gives an energy curve as function of height as shown in Fig. 1(b). For a decreasing ionic strength [I_C, arrow in Fig. 1(b)], the inverse Debye length [κ, Eq. (A3)] decreases and the electrostatic energy increases, pushing the particle away from the surface. From the energy curves the theoretical maximum height displacement Δh of the particle is calculated by taking the minimum and maximum heights for which the energy increases 2.5 k_BT (probability less than 8%) from the energy minimum.

To compare the theoretical height displacements to the measured height displacements, the ionic strength of the buffer solution needs to be determined. The borate buffer is made from mixing 100 mM borax (Sigma-Aldrich) with 100 mM boric acid (Fluka BioChemika) in a ratio of approximately 1:3.5, giving a *p*H of 8.5. A possible reaction for the dissolution of borax is $Na_2B_4O_7 \times 10H_2O \rightarrow 2Na^+ + 2B(OH)_4^- + 2HB(OH)_4$ (due to the low *p*H, reactions involving H^+ can be neglected), which gives an ionic strength of the borate buffer of $I_C = 2M/4.5$, with M the buffer molarity. Using this ionic strength, we fitted the measured height displacements of the particle bound to 590 bp/201 nm DNA [Fig. 3(b)] to the theoretical height displacements and found a good fit for values of $L_{\text{bond}}=200$ nm, Hamaker constant $A=0.7$ k_BT, surface potentials $\psi_p=\psi_s=-50$ mV, and an offset parameter of 5.5 nm (to account for system noise etc.). The data of the remaining particles could be fitted with the same parameters by changing only the bond length L_{bond} to, respectively, 45 nm, 90 nm, and 110 nm for the 36 nm DNA, 48 nm DNA, and 99 nm DNA, see Fig. 3(b). For three out of four particles, the values are very close to the actual bond length. The deviation of the particle bound to 48 nm DNA is probably due to nonuniform optical properties of the particle. We have previously shown that nonuniform optical properties lead to an increase in scattering fluctuations, which is especially noticeable for shorter analyte lengths.[17] We note that the surface potentials (ψ_p, ψ_s) can only be assumed to be constant for a constant *p*H of the buffer, which we verified to be the case for the dilutions used in our experiments.

If borax also dissolves into divalent ions ($Na_2B_4O_7 \cdot 10H_2O \rightarrow 2Na^+ + B_4O_5(OH)_4^{2-} + 8H_2O$), the ionic strength increases to $I_C = 3M/4.5$.[24] This increases the values of the surface potentials in the fit to $\psi_p=\psi_r=-80$ mV [taking an electrovalence of $z=2$ in Eq. (A4)], which becomes substantially higher than values usually reported for comparable surfaces.[25,26] For future measurements, it is preferable to use an electrolyte with better defined ionic strength. Additionally, more research needs to be done on the exact surface potentials of both particle and surface and the influence of the ionic strength and the *p*H on the surface potentials.[25,26]

The model combining the van der Waals and electrostatic energy with a hard boundary energy for the bond thus accounts well for the measured height displacements. We calculated that the energy needed for bending the DNA such that the particle can move toward the surface is indeed negligible (~ 0.2 k_BT) (Ref. 17) compared to the electrostatic energy. It should be noted that for longer DNA probably an addition to the model is required to account for the energy needed to stretch the DNA.[10] It may be possible that the buffer conditions also influence the behavior of the DNA itself. Manning[27] described a model to determine the persistence length of dsDNA and summarized experimental data from literature. They report values for the persistence length increasing from 50 to 130 nm for salt concentrations down to 1 mM. We calculated that even these high persistence lengths do not lead to significant bending energies and, therefore, do not considerably change the model (estimated change in maximum displacement between 0.2 and 2 nm).

IV. CONCLUSIONS

We have demonstrated a technique to modulate the height of bound particle labels in an evanescent wave biosensor by exchanging the buffer. We showed that the intensity of the beam reflected from the sensor surface increases for decreasing ionic strength. This can be explained by an increase in the electrostatic force repelling particles from the surface and out of the evanescent field. Experiments with three different analytes showed that the magnitude in signal change was smallest for troponin and largest for 290 bp DNA. In addition, we measured the fluctuations in scattered intensity of individual particles and saw that the intensity histograms became narrower for lower ionic strengths, with a peak shifting toward lower intensities, corresponding to larger heights. Finally, we described a model to quantitatively analyze the measured height displacements, and found that the model could fit the measured data for particles bound to four different DNA lengths by only changing the bond length parameter. In future biosensors, height manipulation of bound particle labels may lead to improved detection limits and higher detection specificity.

ACKNOWLEDGMENTS

This work was partially funded by the NanoNed program of the Dutch Ministry of Economic Affairs.

APPENDIX: ELECTROSTATIC AND VAN DER WAALS INTERACTION

The interaction energy between a particle and a surface mainly consists of the van der Waals interaction and the electrostatic interaction, which together form the DLVO theory named after Derjaguin and Landau, Verwey and Overbeek.[24] The van der Waals energy between a spherical particle and a flat surface is given by

$$E_{\mathrm{vdw}} = -1/6A\left[\frac{R}{h} + \frac{R}{h+2R} + \ln\left(\frac{h}{h+2R}\right)\right], \tag{A1}$$

with A the Hamaker constant of the particle-fluid-surface combination, R the particle radius, and h the distance between the particle bottom and the surface. The electrostatic energy between the particle and the surface is given by

$$E_{es} = ZR \cdot \exp(-\kappa h). \tag{A2}$$

In this equation κ is the inverse Debye length given by

$$\kappa = \sqrt{\frac{2000e^2 N_A I_C}{\varepsilon_o \varepsilon_r k_B T}} \tag{A3}$$

and Z is a constant given by

$$Z = 64\pi\varepsilon_0\varepsilon_r\left(\frac{k_B T}{e}\right)^2 \tanh\left(\frac{ze\psi_p}{4k_B T}\right)\tanh\left(\frac{ze\psi_s}{4k_B T}\right), \tag{A4}$$

with e the elementary charge, N_A Avogadro's number, I_C the ionic strength of the fluid, ε_0 the dielectric permittivity of free space, ε_r the relative permittivity of the fluid, $k_B T$ the thermal energy, z the electrolyte valence, and ψ_p and ψ_s the surface potentials of, respectively, the particle and the surface.

[1] M. Seydack, Biosens. Bioelectron. **20**, 2454 (2005).
[2] C. R. Tamanaha, S. P. Mulvaney, J. C. Rife, and L. J. Whitman, Biosens. Bioelectron. **24**, 1 (2008).
[3] D. Wild, *The Immunoassay Handbook*, 3rd ed. (Elsevier, Amsterdam, 2005).
[4] D. M. Bruls, T. H. Evers, J. A. H. Kahlman, P. J. W. van Lankvelt, M. Ovsyanko, E. G. M. Pelssers, J. J. H. B. Schleipen, F. K. de Theije, C. A. Verschuren, T. van der Wijk, J. B. A. van Zon, W. U. Dittmer, A. H. J. Immink, J. H. Nieuwenhuis, and M. W. J. Prins, Lab Chip **9**, 3504 (2009).
[5] L. Han, B. Lui, S. Blumberg, J. F. Beausang, P. C. Nelson, and R. Phillips, in *Mathematics of DNA Structure, Function and Interactions*, edited by C. J. Benham, S. Harvey, W. K. Olson, D. W. Sumners, and D. Swigon (Springer, New York, 2009), Vol. 150, p. 123.
[6] D. A. Schafer, J. Gelles, M. P. Sheetz, and R. Landick, Nature (London) **352**, 444 (1991).
[7] A. Ashkin, J. M. Dziedzic, J. E. Bjorkholm, and S. Chu, Opt. Lett. **11**, 288 (1986).
[8] A. A. Deniz, S. Mukhopadhyay, and E. A. Lemke, J. R. Soc., Interface **5**, 15 (2008).
[9] A. N. Kapanidis and T. Strick, Trends Biochem. Sci. **34**, 234 (2009).
[10] C. Bustamante, Z. Bryant, and S. B. Smith, Nature (London) **421**, 423 (2003).
[11] M. Panhorst, P.-B. Kamp, G. Reiss, and H. Brückl, Biosens. Bioelectron. **20**, 1685 (2005).
[12] H. Shang and G. U. Lee, J. Am. Chem. Soc. **129**, 6640 (2007).
[13] I. D. Vilfan, J. Lipfert, D. A. Koster, S. G. Lemay, and N. H. Dekker, *Handbook of Single-Molecule Biophysics* (Springer, New York, 2009), p. 371.
[14] S. P. Mulvaney, C. L. Cole, M. D. Kniller, M. Malito, C. R. Tamanaha, J. C. Rife, M. W. Stanton, and L. J. Whitman, Biosens. Bioelectron. **23**, 191 (2007).
[15] G. Zocchi, Biophys. J. **81**, 2946 (2001).
[16] D. Leckband, Annu. Rev. Biophys. Biomol. Struct. **29**, 1 (2000).
[17] K. van Ommering, M. Koets, R. Paesen L. J. van IJzendoorn, and M. W. J. Prins, J. Phys. D (accepted).
[18] M. Singh-Zocchi, S. Dixit, V. Ivanov, and G. Zocchi, Proc. Natl. Acad. Sci. U.S.A. **100**, 7605 (2003).
[19] D. C. Prieve, Adv. Colloid Interface Sci. **82**, 93 (1999).
[20] G. Zocchi, ChemPhysChem **7**, 555 (2006).
[21] M. Koets, T. van der Wijk, J. T. W. M. van Eemeren, A. van Amerongen, and M. W. J. Prins, Biosens. Bioelectron. **24**, 1893 (2009).
[22] K. van Ommering, P. A. Somers, M. Koets, J. J. H. B. Schleipen, L. J. van IJzendoorn, and M. W. J. Prins, J. Phys. D: Appl. Phys. **43**, 155501 (2010).
[23] S. Blumberg, A. Gajraj, M. W. Pennington, and J.-C. Meiners, Biophys. J. **89**, 1272 (2005).
[24] J. N. Israelachvili, *Intermolecular and Surface Forces*, 2nd ed. (Academic Press, London, 1991).
[25] X. J. A. Janssen, A. van Reenen, L. J. van IJzendoorn, A. M. de Jong, and M. W. J. Prins (to be published).
[26] R. Wirix-Speetjens, W. Fyen, K. Xu, J. De Boeck, and G. Borghs, IEEE Trans. Magn. **41**, 4128 (2005).
[27] G. S. Manning, Biophys. J. **91**, 3607 (2006).